

Measuring the Diameter of Nanofibers Extracted from Polyblend Fibers Using FCM Clustering Method

Neda Dehghan, Pedram Payvandy, and Mohammad Ali Tavanaie

Abstract—Extracting two component nanofibers from blend polymers is one of the interesting methods of industrial production of nanofibers. Knowing the morphology of nanofibers structure is essential for improving their efficiency. Fiber diameter is one of the major structural properties, which is typically determined by manual measuring methods. However, manual fiber diameter calculation is a tedious and time consuming task as well as being sensitive to human errors. Therefore, an accurate and automated technique to measure the diameter of fibers is desired. In recent years, image processing methods have been commonly used to measure the diameter of nanofibers. In this study, image segmentation based on Fuzzy Clustering Method (FCM) and Distance Transform Method (DTM) was used to measure the diameter of nanofibers extracted from blend fiber. The diameter of nanofibers was calculated using proposed method and results were compared with other image processing algorithms and the manual method. The presented results showed that the FCM approach can be helpful for measuring the nanofiber diameter within a fibrous network.

Keywords: diameter, FCM, image processing, nanofiber

I. INTRODUCTION

Nanofibers are defined as fibers with diameters less than 100 nanometers or fibers that are less than 1 micron in diameter with specific properties. These special properties include: flexibility, extremely small pore size, and large surface area per unit mass. These characteristics lend nanofibers to many innovative applications including artificial organ components, tissue engineering, implant materials, drug delivery systems, wound dressings, and medical textile materials which require high accuracy and efficiency in production.

In the recent years, nanofibers have been produced in laboratory scale by a number of processing techniques, including drawing, template synthesis, phase separation, self-assembly, electrospinning, and extraction from polymer blend fibers. There are many limits and non-uniformity of the process in the nanofiber producing methods. Nanofiber production from blend fibers is a new approach that takes advantage of the properties such as higher production speed, lower production cost and flexibility in the production process [1-5].

Fiber diameter is one of the major morphological properties of nanofibers, which is typically determined by manual measurement of the diameter of randomly selected fibers on scanning electron microscopy (SEM) images. However, by increasing the number of the images, manual fiber diameter determination becomes a time consuming task and the probability of human errors increases. So, automatic methods have been proposed in order to replace the manual techniques [6-14].

Shin *et al.* [7] applied an image processing method to determine the diameter of electrospun nanofibers. They used Distance Transform Method (DTM) but with a manual thresholding. Ziabari *et al.* [8] used local threshold method to threshold SEM images, and suggested a new DTM to measure the diameter of electrospun nanofibers. The measurement was conducted more accurately by specifying the intersection of fibers and removing them from the image. Maleki *et al.* [10] suggested a direct tracking method for measuring the diameter of nanofibers, which is also mentioned in other studies [15,16]. It has been clarified by those studies that DTM generally has more precise results than direct tracking method. But in the case of low density electrospun nanofiber images, direct tracking methods can show more accurate results [16]. Hotaling *et al.* [14] introduced a new method based on super pixel algorithm to calculate nanofiber diameters. In their study, the algorithm was validated by using digital binary synthetic images and steel wire SEM images with known diameters.

Due to capturing conditions there were some drawbacks in many of the SEM images such as low local contrast, changes of light intensity, noise, etc. [17,18]. Since these mentioned problems seriously affect the thresholding process, some segmentation methods based on clustering have been considered in order to reduce cited deficiencies. K-means [19,20] and Fuzzy Clustering Method (FCM) are two considered methods for image segmentation [21].

Nock *et al.* [22] suggested a segmentation algorithm based on a model of image generation which captures the idea that grouping is an inference problem. This approach can be efficiently approximated in linear time/space, leading to a fast segmentation algorithm tailored to processing images described using most common numerical pixel attribute spaces.

In this study, an image processing method based on FCM is proposed for thresholding blend fiber SEM images. The results of the proposed method were compared with the values measured manually and the results of other image processing algorithms such as global

N. Dehghan, P. Payvandy, and M. A. Tavanaie are with the Textile Engineering Department, Faculty of Engineering, University of Yazd, Yazd, Iran. Correspondence should be addressed to P. Payvandy (e-mail: Peivandi@yazd.ac.ir)

[7,13], local [8,9], and K-means [19,23]. In addition, the proposed DTM was compared with a newly introduced method named super pixels algorithm [14].

II. PROBLEM STATEMENT

Physical and mechanical properties of nanofiber webs and nonwoven textile are not only dependent on the properties of their materials, but also on their structural characteristics. Fiber diameter is one of the major structural properties of nanofiber webs. In recent years, image processing methods have been developed to measure some properties such as: fiber orientation [24,25], fiber uniformity [26], fiber diameter [5,7-10,23], and nanofiber web pore size [27-29]. The flowchart of measuring nanofiber properties using image processing is illustrated in Fig. 1.

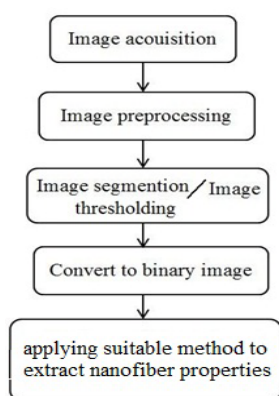


Fig. 1. Flowchart of determining nanofiber properties using image processing.

Image acquisition is the first step of image processing which strongly affects the result. The second step is image preprocessing. Since the image processing is extremely sensitive to noise, cleaning up the noise and enhancing the contrast of the image is necessary before the segmentation. For this purpose smoothing filters (average filter or median filter) or denoising filters (wavelet filter) are used.

Thresholding techniques can be generally categorized into global and local thresholding. Global thresholding selects a single threshold value from the histogram of the image, while in local thresholding method, the threshold is chosen for each sub image [30].

The nanofibers in an SEM web image are placed in layers; the upper layers are lighter and fibers in the lower layers are darker. As a result, the SEM images of nanofibers have two different light intensities. In the routine methods of measuring, there is a possibility of removing some of the upper or lower layers of nanofibers from SEM images. But in the thresholding (segmentation method), the images are segmented to more than two parts, one of which belongs to the background image. Other parts make the object (nanofiber) in the image by merging together. This reduces the chance of removing fibers and also decreases the creation of errors in the measuring process. As can be seen in Fig. 2 an SEM image contains nanofibers with lighter and darker intensity.

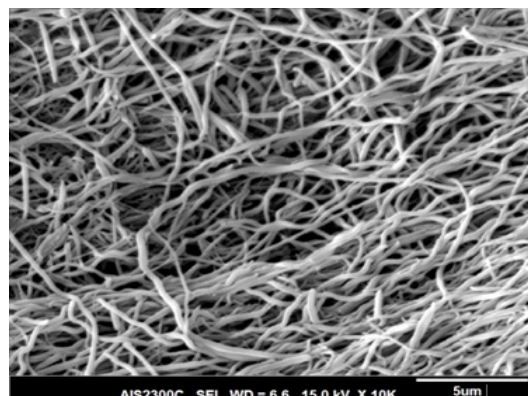


Fig. 2. An example of different light intensities in a nanofiber SEM image [23].

III. MATERIALS

To evaluate the performance of the proposed method of measuring the diameter, nanofibers with different diameters were produced. Blend fibers are two-component fibers which have two distinct polymeric materials in the form of fibrils and a matrix. Blending immiscible polymers often results in two-phase structures, in which the matrix component form the matrix phase and the sub-component form the dispersed phase. The dispersed phase can have different forms and one of them is the fibril form. Extracting nanofibrils from films and blend fibers is one of the methods of producing nanofibers [1-5].

In this study, industrially produced blend fibre of PP/PBT with low orientation (LOY) was used. The PP/PBT fibre was melt spun under industrial conditions at Aliaf Co. (Tehran) at a low spinning speed. This machine was equipped with an extruder, model 4E6 (Barmag Co., Germany), with a screw length to diameter ratio of 24; and included a gear pump with a capacity of 0.8 ml per round (German Zenite Co.), a spinneret with circular holes (German Elmer Co.), and a winding machine (IWKA, Germany). The melt spinning specifications of PP/PBT blend fibers under industrial conditions include: extruder screw speed of 20 rpm; final temperature of extrusion, spinning head and spinneret of 260°C; melt pressure of 90 bar at output of the extruder; gear pump speed of 8 rpm; cooling air temperature of 19°C; cooling air speed of 0.3 m min⁻¹; winding speed of 800 m min⁻¹; and spinneret hole number of 17.

The drawing process was carried out up to the maximum drawability of the fiber samples (draw ratio of 4). Twelve draw ratios were applied to the fibers from 1.25 to 4 at intervals of 0.25. The drawing process was conducted using a tensile testing machine manufactured by SDL International Ltd/Shirley Development Ltd (SDL micro 350, Manchester, UK), the performance of which is based on a constant rate of elongation and a load cell of 10 kgf.

By dissolving the polypropylene matrix phase of the blend fiber using xylene solvent, polybutylene terephthalate (PBT) dispersed phase was obtained as a layer of nanofibers. Boiling xylene was used to dissolve polypropylene in order to extract the nanofiber layers from blend fibers. For each sample 10-15 ml of xylene was used.

Based on the experiments conducted at different times, and observing the SEM images, the best time for dissolving the matrix phase component was 30 minutes. The layers obtained from the extraction were placed at room temperature for 24 hours until they were completely dried and the solvent was removed.

The diameter of the dispersed phase particles were reduced when an increase in draw ratio occurred, as shown in Fig. 3. In the image of the undrawn nanofiber layer, the shape of the dispersed phase particles is almost ellipsoidal. By an increase in draw ratio, the ellipsoidal shape of the particles is converted into completely drawn shapes.

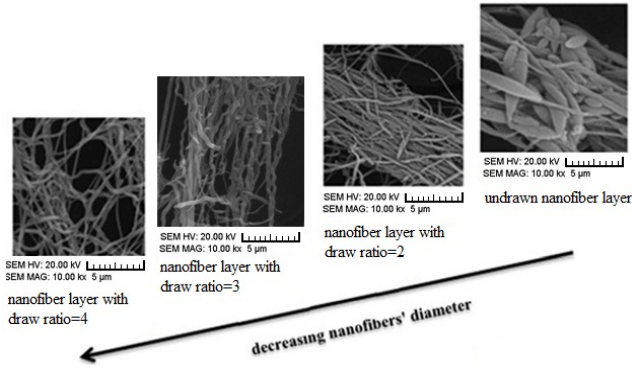


Fig. 3. Deformation of dispersed phase with increase in draw ratio.

In order to study the morphology of the nanofiber layer extracted from blend fibres, scanning electron microscopy (Tescan Co, Czech) was used. Nanofiber images of blend fibres were captured with magnifications of 5000, 10000, 15000 and 30000. At each drawing ratio four SEM images were taken in different magnifications and totally 52 SEM images were achieved. Since all taken pictures were not qualified enough, 40 images were chosen among them.

IV. METHODS

A. Thresholding Methods

Thresholding is the process of converting a gray scale image to a binary image using an optimum threshold value. This is a process of partitioning an image into object pixels and background pixels. A pixel is considered an object pixel if the pixel value is greater than a certain threshold value. The methods used for thresholding are global thresholding and local thresholding, or thresholding based on clustering segmentation algorithms such as: K-means and FCM.

When the pixel intensity distribution of the objects and the background are separate one can use the global thresholding on entire image [30]. Local thresholding is used to compensate the background non-uniform illumination by dividing the original image into sub images, and the global thresholding is applied to each of the sub images [31].

Clustering is a branch of data analysis which assigns the data to a number of predetermined clusters using common data features with no need to the default data. Cluster is a set of objects which are similar, and dissimilar to other objects. Different factors can be considered for similarity,

one of which is a distance factor that can be used for clustering. Then, the closer objects are regarded as one cluster. K-means algorithm is one of the most simple and common clustering algorithms [32].

B. Fuzzy C-Means (FCM)

One of the most important and applicable clustering algorithms is FCM. Pixels in this algorithm are divided into c clusters. This method was developed by Bezdek *et al.* [33]. The objective function for this algorithm is defined as following:

$$J = \sum_{j=1}^N \sum_{i=1}^C u_{ij}^m d_{ij}^2 d_{ij} = |x_j - v_i| \quad (1)$$

where $X=(x_1, x_2, \dots, x_N)$, is the image characteristic while N denotes the number of the image pixels, U_{ij} denotes the indicative of pixel membership x_j in the first cluster or the second, v_i is the center of the first or the second cluster, and d_{ij} indicates the similarity value (distance) of the sample from the cluster center which can use any function indicative of sample similarity and cluster center. In the above formulae, m denotes an actual number greater than 1. In this paper $m=2$ was considered. Objective function J will be minimum, when pixels are closer to their cluster centers and have a high membership value. Pixels farther than the centers have a low membership value.

Algorithm steps:

1. An initial amount for c and m , and the accuracy of ε and initial clusters are assumed.
2. The membership degree matrix, $U(0)$, is calculated and the counter $t = 1$.
3. The cluster center matrix is updated by membership degree matrix of the following equation:

$$v_i = \frac{\sum_{j=1}^n u_{ij}^m x_j}{\sum_{j=1}^n u_{ij}^m}, i = 1, 2, \dots, c \quad (2)$$

4. The U membership degree matrix is updated and $t = t + 1$.
5. The following equation is applied:

$$u_{ij} = \left[\sum_{k=1}^c \left(\frac{d_{ij}}{d_{kj}} \right)^{\frac{2}{m-1}} \right]^{-1} \quad (3)$$

6. If $|U^{(t+1)} - U^{(t)}| \leq \varepsilon$, the algorithm ends, otherwise returns to step 2.

Finding the best clusters is a cluster validation problem [34]. Therefore, many studies have been carried out by researchers in order to obtain the best clusters [35-37]. Clustering validation index mainly uses two criteria of compression and dispersion to evaluate clustering [38-41]. These indices calculate the compression in each cluster and separation between cluster centers. Some of the famous cluster validation indices are Dunn index [38], Davies Bouldin Index [39], index validation of the root mean

square deviation [40], SD validation index [41], etc. In this study, Davies-Bouldin index is used to evaluate the clusters. The main goal of image segmentation is to divide an image into parts that have strong correlations with objects or areas of the image.

The aim is to separate the image of nanofibers from their background using segmentation methods.

To determine the optimum number of clusters in the clustering methods firstly the different number of clusters (up to 6) is chosen. Then the binary image result of each of them is compared to the original images using Mean Structural Similarity Index Method (MSSIM) index. The results showed that the maximum MSSIM index value happen when the number of clusters is 3. So, in order to classify images of nanofibers for image segmentation in both K-means and FCM methods, a numerical value of 3 was assigned to the number of the clusters (C). Therefore the nanofiber images could be divided according to different light intensity layers.

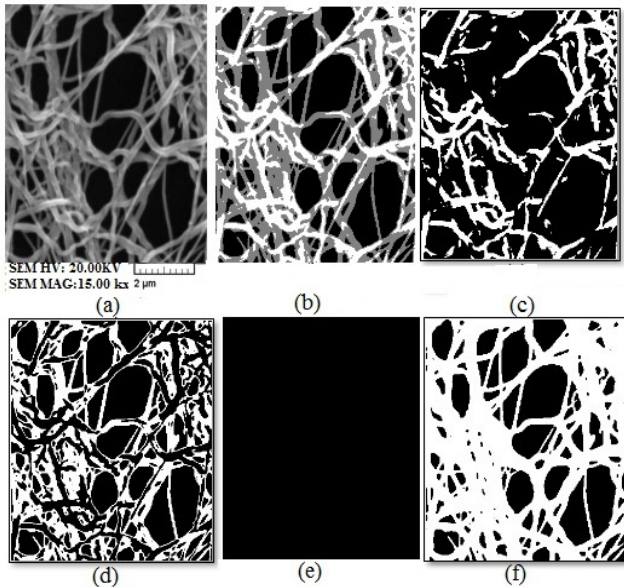


Fig. 4. a) An original image of nanofibers, b) FCM segmented image, c) FCM segmented layer1, d) FCM segmented layer 2, e) FCM segmented layer 3, f) thresholding image obtained from adding c and d.

By dividing the image into 3 clusters, the cluster with more central intensity was considered as the first layer. This cluster included more visible parts of the nanofibers due to their position. The one with lowest light intensity was considered as the background and was named the third layer. The remained cluster was considered as the second layer in which the cluster center was in the middle of the first and the third cluster centers. Fig. 4 shows a sample of nanofiber image segmentation.

It can be observed from Fig. 4(f) that nanofiber images are formed from two different light intensities in combination. The two-part created nanofiber image, obtained from segmentation, performed better than that obtained from usual threshold method. The amount of loss of image useful information should be checked regardless of the type of the thresholding method. For this purpose an

image quality evaluation technique is used which is mentioned in the next part of the paper.

C. Structural Similarity Index Method (SSIM)

The Structural Similarity Index is a method for calculating the similarity between two images. The SSIM index can be viewed as an indicator for assessing the quality of an image compared to other images [42].

This criterion of SSIM is measured on different frames of images. Measurement between two frames x and y in $N \times N$ size is as follows:

$$SSIM(x, y) = \frac{(2\mu_x \mu_y + c_1)(2\sigma_{xy} + c_2)}{(\mu_x^2 + \mu_y^2 + c_1)(\sigma_x^2 + \sigma_y^2 + c_2)} \quad (4)$$

In Eq. (4), μ_x and μ_y denote the means, and σ_x and σ_y are the the variances of x and y respectively, and σ_{xy} is the covariance between x and y . The constants C_1 , C_2 are calculated as follows:

$$C_1 = (K_1 L)^2 \quad (5)$$

$$C_2 = (K_2 L)^2 \quad (6)$$

where $K_1=0.01$, $K_2=0.03$ and L is the total possible intensity levels (255 for 8-bit grayscale images). The quality evaluation of the whole image equals to:

$$MSSIM(X, Y) = \frac{1}{M} \sum_{j=1}^M SSIM(x_j, y_j) \quad (7)$$

In Eq. (7), X indicates the basic image (original) and Y is the output image of each algorithm which is supposed to be compared. x_j , y_j are the contents of the j^{th} local frame, and M is the number of local frames in image [42]. In this study the frame is displaced pixel-by-pixel on the image. So M is equal to the number of the pixels in the image.

According to the image processing flowchart which is shown in Fig. 1, after an image converts to the binary form by thresholding techniques, a suitable measuring method will be considered depending on the parameters that are desired to determine. In this study, the aim is to calculate the nanofiber diameter, therefore, the measurement methods used in this research are introduced in the following part.

D. Diameter Measurement Methods

1) Distance transform method (DTM)

The distance transform is an operation which is applied to a binary image consisting of 1 s and 0 s corresponding to objects and background, respectively. For each pixel in the binary image, the corresponding pixel in the distance transformed image has a value equal to the minimum distance between that pixel and the closest object pixel, that is, the distance from that pixel to the nearest non-zero valued pixel [43,44].

Three common distance methods are used in order to measure the distance between the pixels :city block, chessboard and Euclidean. Fig. 5 shows these methods. The city block distance gives the length of a path between

the pixels according to a 4-connected neighborhood (moving only in horizontal and vertical directions), Fig. 5(b). The city block distance between (x_1, y_1) and (x_2, y_2) is given by:

$$Distance_{cityblock} = (|x_1 - x_2| + |y_1 - y_2|) \quad (8)$$

In contrast, the chessboard distance metric measures the path between the pixels based on an 8-connected neighborhood (diagonal move is also allowed), Fig. 5(c). This metric is given by:

$$Distance_{chessboard} = Max(|x_1 - x_2|, |y_1 - y_2|) \quad (9)$$

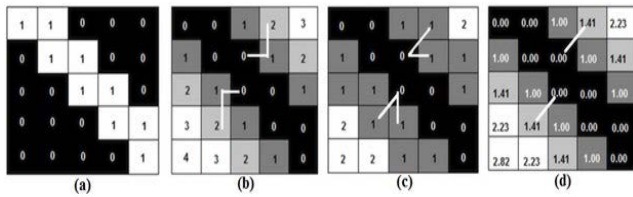


Fig. 5. a) A small binary image and its distance obtained by; b) city block, c) chessboard, d) Euclidean.

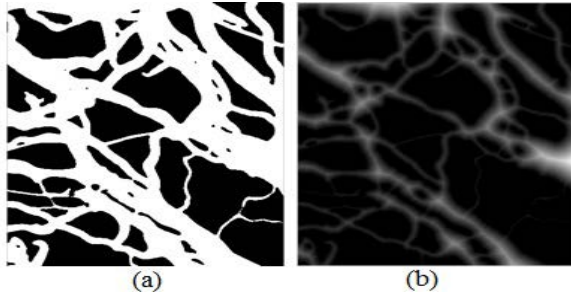


Fig. 6. a) A sample nanofiber binary image, b) the image obtained by Euclidean distance.

In the city block metric, distances in the diagonal direction are longer, resulting in diamond-shaped structures. If a chessboard metric is used, square-shaped structures are obtained [44]. Even though they could be used in certain applications, the Euclidean metric is more practical and relevant, since it is the only one that preserves the isotropy of the continuous space, Fig. 5(d) [45]. The Euclidean distance, which is the straight line distance between two pixels, is defined as:

$$Distance_{euclidean} = \sqrt{(x_1 - x_2)^2 + (y_1 - y_2)^2} \quad (10)$$

Fig. 6 shows an example of using Euclidean distance on a nanofiber binary image.

2) Super pixel diameter determination

The super pixel algorithm divides the area of all the fibers in an image by the total length of all the fibers' centerlines. This transforms the unit measurement size from a single pixel to a new value called the "super pixel" diameter which is equal to the mean fiber diameter. To obtain this calculation, white pixels from binary images were summed for total fiber area in each image. The length

of the centerlines was calculated and the total area of fibers was divided by the length. This calculation gave the approximation of the super pixel diameter. The super pixel name was chosen because the fiber area (in pixels) was divided by the centerline lengths (in pixels), producing a unit-less value that is equivalent to a transformed (larger) pixel unit, equivalent to the mean fiber diameter [14].

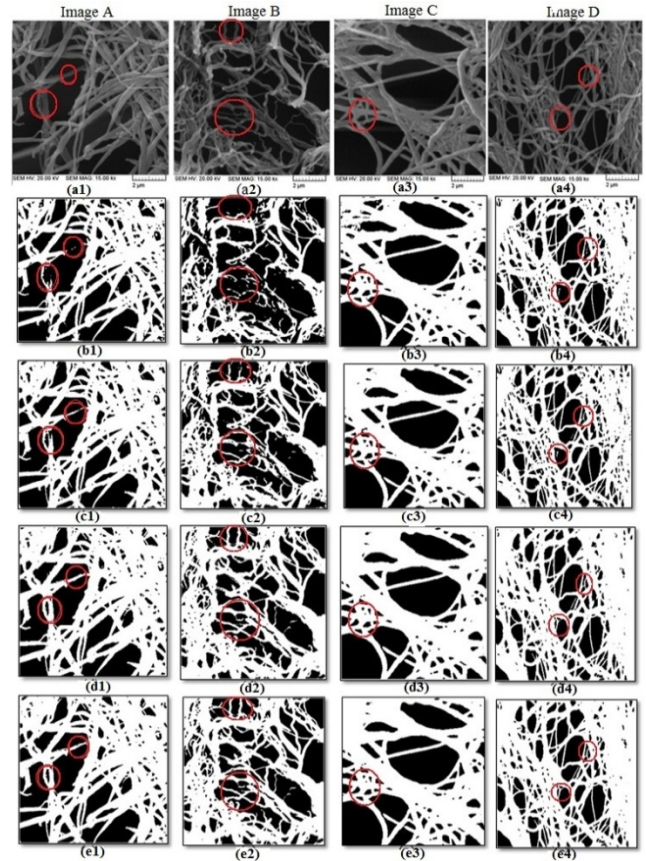


Fig. 7. Nanofiber images: A) undrawn nanofiber, B) nanofiber with draw ratio of 2, C) nanofiber with draw ratio of 3, D) nanofiber with draw ratio of 4. (a1-a4): original images, (b1-b4): Global thresholding, (c1-c4): Local thresholding, (d1-d4): K-means thresholding, (e1-e4): FCM thresholding.

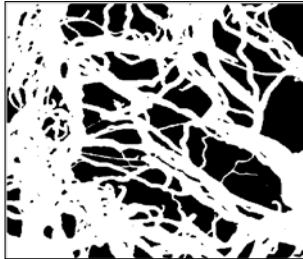
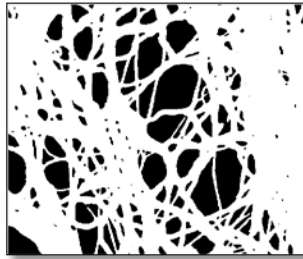
3) Manual measurement

A manual method is a commonly-used method for measuring the diameter of fibres. First, a scale was set; then, pixels located between two edges of the vertical axis were counted. The number of pixels was converted to nanometer (nm) and the results were reported. Depending on the condition of an image, 30 to 100 measurements could be made within it.

V. RESULTS AND DISCUSSION

In this study, for the first step, all nanofiber images were denoised using a wavelet transform filter. Next all introduced thresholding methods were applied on images. The results of the thresholding methods for four samples of nanofiber SEM images are illustrated in Fig. 7. For better visual comparison the difference in performance of thresholding techniques are marked with red circles in Fig 7.

TABLE I
QUALITY ASSESSMENT OF DIFFERENT METHODS IN COMPARISON WITH BASIC METHOD

quality assessment of algorithms quality to image		algorithm	MSSIM index	quality assessment of algorithms quality to image		algorithm	MSSIM index
A				B			
		Global	0.9895			Global	0.9881
		Local	0.9986			Local	0.9969
		K-means	0.9995			K-means	0.9980
		FCM	0.9999			FCM	0.9988
quality assessment of algorithms quality to image		algorithm	MSSIM index	quality assessment of algorithms quality to image		algorithm	MSSIM index
C				D			
		Global	0.9789			Global	0.9898
		Local	0.9883			Local	0.9963
		K-means	0.9995			K-means	0.9983
		FCM	0.9991			FCM	0.9999

Considering that manually finding of the best thresholding method for all captured images is not possible, the MSSIM index is applied in this case. The results of MSSIM for the sample images are shown in Table I.

It should be noted that the MSSIM index value is extremely influenced by the number of similar pixels in threshold and original images. And since the threshold image of the original image is very similar to the original image, the MSSIM index is near to 1. In Table II the results of MSSIM for all images are listed.

TABLE II
MEAN QUALITY ASSESSMENT OF DIFFERENT ALGORITHMS FOR ALL THE IMAGES

Methods	global	local	K-means	FCM
Mean	0.9978	0.9972	0.9990	0.9993
Std	3.2×10^{-3}	5.1×10^{-3}	8.8×10^{-4}	6.2×10^{-4}

As it is clear in Tables I and II, the FCM for these images gives the better results than other methods, therefore, it is chosen as the target thresholding method. As it is illustrated in Table II, all methods are approximately the same. There is a little difference in the MSSIM index method which is related to the fibers boundary in the images, so it has an effect on the results of diameter determination methods, as it can be seen in Table III.

As can be seen in Table III, the mean and standard deviation of diameter of fibers in FCM are in good agreement with that in manual method. The maximum difference between FCM and manual method is 7.61%, while the maximum value for the global method, local method and K-means method is 19.84%, 10.15% and 7.76%, respectively.

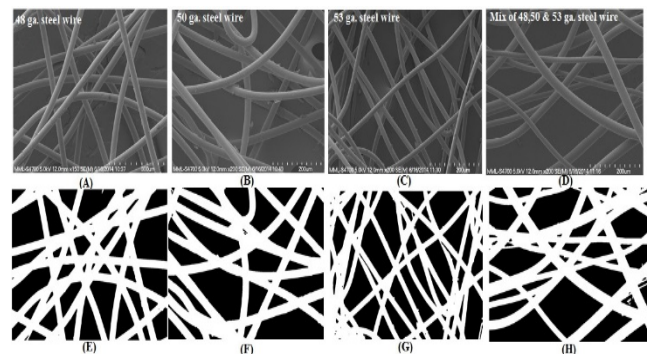


Fig. 8. (A-D): Original SEM images of steel wires, (E-H): segmented SEM micrographs using thresholding techniques available as plugins within Image J/FIJI [14].

In order to validate the proposed DTM, an open access dataset of object images with known object diameter, introduced by Hotaling *et al.* [46], was used. The selected dataset images contained three gauges (48, 50, and 53 ga.) of steel wire. The SEM micrographs of steel wires and their related segmented images are shown in Fig. 8.

The diameter of wires was calculated using the DTM method and the results are shown in Table IV. For a better comparison the results of determining wire diameter using super pixel method were added to Table IV.

Table IV specifies that, there was no significant difference in the method results. For further investigation and in order to determine the more efficient method, 5 simulated images with specified diameter were used [46]. The images contained straight and curved line images with a single width or multiple widths (Fig. 9).

The results of line diameter determination by DTM and super pixel method are compared in Table V.

It can be seen in Table V that the diameters measured by DTM are greater than those measured manually. This may be due to some remaining branches in the skeleton even after pruning. The thicker the line, the higher the possibility of branching during thinning. Although these branches are small, their orientation is typically normal to the fiber axis resulting in widening of the distribution obtained by the DTM.

TABLE III
COMPARISON OF NANOFIBER DIAMETER EXTRACTION BY DESCRIBED METHODS

	M & Std (nm)	Image A	Image B	Image C	Image D
		Manual	Mean	361.34	317.95
	Std	55.290	55.074	39.486	45.393
	Error*	0	0	0	0
Otsu threshold	Mean	392.25	329.57	283.92	162.94
	Std	76.312	55.620	47.479	35.551
	Error*	8.55	3.65	19.84	6.75
Local threshold	Mean	394.53	322.90	249.21	192.49
	Std	72.498	58.487	49.521	27.044
	Error*	9.18	1.55	5.19	10.15
K-means method	Mean	389.40	327.00	246.73	170.00
	Std	68.137	55.931	49.625	33.308
	Error*	7.76	3.15	4.14	2.71
FCM method	Mean	384.23	322.67	244.62	188.04
	Std	73.828	55.321	45.490	30.152
	Error*	6.33	1.48	3.25	7.61

*Error =

$$\left(\frac{\text{mean diameter in manual method} - \text{mean diameter in threshold method}}{\text{mean diameter in manual method}} \right)$$

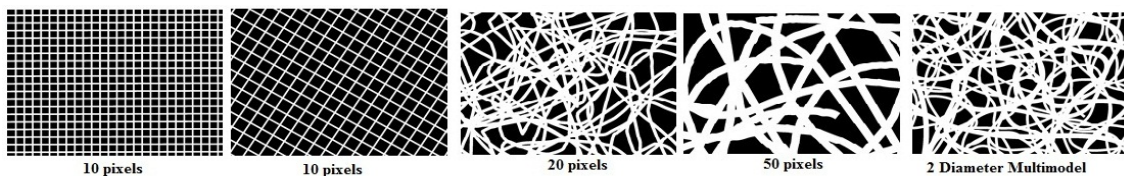


Fig. 9. Simulation images of lines with known width, 10, 10, 20, 50 pixels (single width), 35 and 50 pixels (multi width).

TABLE IV
STEEL WIRE SEM IMAGE ANALYSES USING SUPER PIXEL AND DTM

SEM micrographs steel wire	Real diameter	Super Pixel method (Hotaling <i>et al.</i> , 2015)		DTM												Manual method			
					Global method			Local method			K-means method			FCM method					
		d _{mean} *	Std	Error (%)	d _{mean} *	Std	Error (%)	d _{mean} *	Std	Error (%)	d _{mean} *	Std	Error (%)	d _{mean} *	Std	Error (%)	d _{mean} *	Std	Error (%)
Original image of 48 ga.	31.084	28.62	0.84	7.32	27.011	7.10	13.10	28.219	8.65	9.21	33.582	6.07	8.03	33.221	4.11	6.87	31.07	1.54	0.04
Original image of 50 ga.	25.65	24.117	4.16	5.97	22.512	5.21	12.23	24.623	4.76	4.00	27.024	3.59	5.35	26.66	2.42	3.93	25.45	1.37	0.7

$$\text{Error} = \left(\frac{\text{real diameter} - \text{mean diameter in all method}}{\text{real diameter}} \right)$$

* d_{mean}: mean diameter

TABLE V

MEAN AND STD OF LINE WIDTHS IN DIGITAL SYNTHETIC IMAGES OBTAINED FROM SUPER PIXEL AND DTM

Digital synthetic images Diameter (pixels)	Super Pixel (Hotaling <i>et al.</i> , 2015b).			DTM		
	Mean (pixels)	Std	Error (%)	Mean (pixels)	Std	Error (%)
5	5.19	0.13	3.8	5.3	0.8	6
10	9.76	0.10	2.4	10.2	1.17	2
20	17.93	2.56	10.35	21.38	3.6	6.9
50	45.08	0.64	9.84	51.86	5.08	3.72
100	94.94	13.93	5.06	110.46	8.80	10.26

Also in DTM the diameter measurement errors increase at resolutions less than 10 pixels and more than 50 pixels. Maybe because at resolutions less than 10 pixels the number of the remaining branches increases while in resolutions more than 50 pixels the size of the remaining branches rise. According to the diameter errors in Table I the accuracy of DTM is greater than super pixel method in resolutions between 10 to 50 pixels. In the SEM images of produced nanofibers, the resolution of fiber images is in the range of which DTM presents more accurate results.

So this method was selected to determine the fiber diameter in the images. The diameter frequency distribution of sample images determined by distance and manual methods are shown in Fig. 10.

Also DTM and manual methods were used to analyze 40 nanofiber SEM images in all draw ratios (Fig. 11).

Fig. 11 shows the mean diameter distribution of fibers in different drawing ratios. It is obvious that this proposed method is reliable in measuring the mean fiber diameter correctly, and manual measurements of nanofiber diameters are not statistically different from DTM.

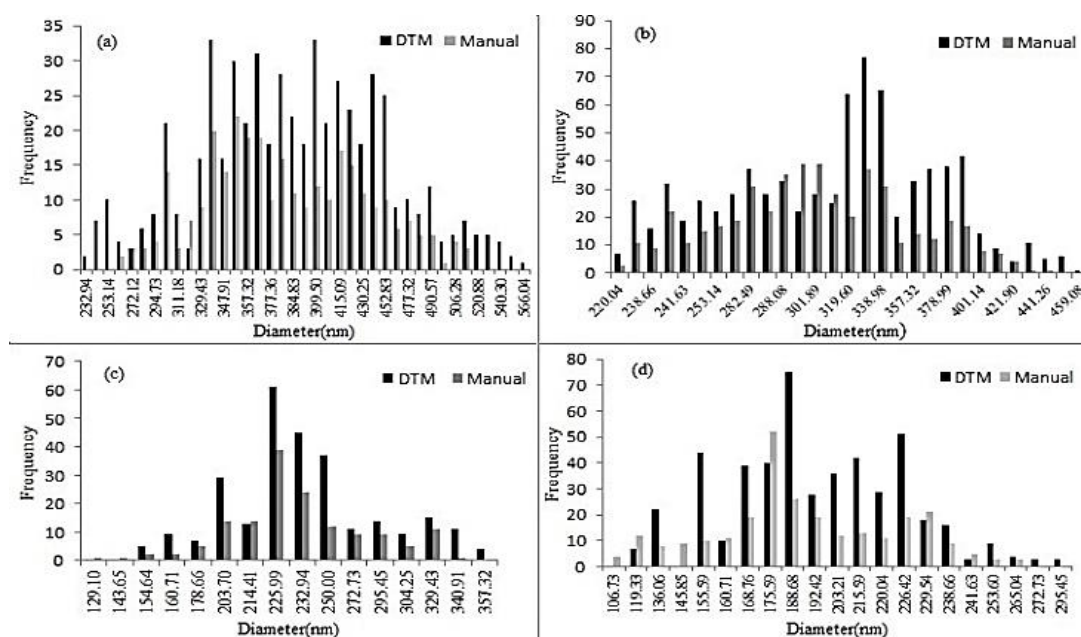


Fig. 10. Diameter distribution of nanofibers produced from blend fibers, obtained from manual method and FCM- DTM; a) undrawn, b) with draw ratio of 2, c) with draw ratio of 3, d) with draw ratio of 4.

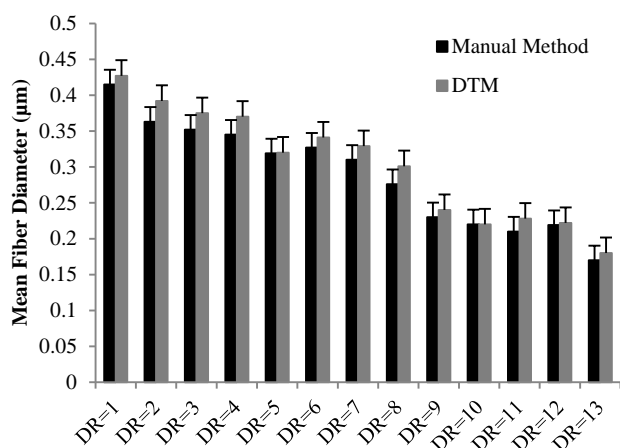


Fig. 11. The mean diameter distribution of fibers in different drawing ratios calculated by manual method and DTM.

VI. CONCLUSION

One of the most nanofiber industrial production methods is extracting nanofibers from blend fibers. Knowing the morphology of nanofiber structures is very important for improving the efficiency of nanofibers. Traditional methods are very time consuming in determining the pore size, measuring diameters, and also precise measuring of the properties, therefore, moving toward quick and accurate methods such as image processing is inevitable. In this paper an image processing method based on FCM was proposed for measuring the diameter of nanofibers extracted from blend fibers. Then results of this algorithm were compared with other image processing algorithms such as global, local, K-means and manual method. Visual and computational results obtained from image quality indicators, MSSIM, revealed that FCM was a more

suitable method for thresholding the images of nanofibers that were analyzed in this report.

The validity of the diameter detection methods were tested using simulated images, and SEM images of steel wires. The result of distance transform and super pixel methods were close to true values on the simulated and steel wire images. But in the resolutions that images were taken, the DTM performed more accurately. As it could be observed, the obtained frequency distribution results of FCM, DTM and manual methods were very close at all draw ratios. This indicates the accuracy of this technique and its priority over other time consuming manual methods.

REFERENCES

- [1] M. V. Tsebenko, A. V. Yudin, T. I. Ablazova, and G. V. Vinogradov, "Mechanism of Fibrillation in The Flow of Molten Polymer Mixtures", *Polymer*, vol. 17, no. 9, pp. 831-834, 1976.
- [2] L. A. Utracki, M. M. Dumoulin, and P. Toma, "Melt Rheology of High Density Polyethylene/Polyamide6 Blends", *Polym. Eng. Sci.*, vol. 26, no. 1, pp. 34-44, 1986.
- [3] A. D. Padsalgikar and M. S. Ellison, "Modeling Droplet Deformation in Melt Spinning of Polymer Blends", *Polym. Eng. Sci.*, vol. 37, no. 36, pp. 994-1002, 1997.
- [4] Q. Xinga, M. Zhu, Y. Wang, Y. Chen, Y. Zhang, J. Piontech, and H. Adler, "In Situ Gradient Nano-Scale Fibril Formation During Polypropylene/Polystyren (PP/PS) Composite Fine Fiber Processing", *J. Polym.*, vol. 46, no. 14, pp. 5406-5416, 2005.
- [5] N. Dehghan, M.A. Tavanaie, and P. Payvandy, "Morphology Study of Nanofibers Produced by Extraction From Polymer Blend Fibers Using Image Processing", *Korean. J. Chem. Eng.*, vol. 32, no. 9, pp. 1928-1937, 2015.
- [6] T.S. Courtney, M. Sacks, J. Stankus, J. R. Guan, and W. Wagner, "Design and analysis of tissue engineering scaffolds that mimic soft tissue mechanical anisotropy" *Biomaterials*, vol. 27, no. 19, pp. 3631-3638, 2006.
- [7] E. H. Shin, K. S. Cho, M. H. Seo, and H. Kim, "Determination of Electrospun Fiber Diameter Distributions Using Image Analysis Processing". *Macromol. Res.*, vol. 16, no. 4, pp. 314-319, 2008.

- [8] M. Ziabari, V. Mottaghtalab, and A. K. Haghi, "Distance Transform Algorithm For Measuring Nanofiber Diameter", *Korean. J. Chem. Eng.*, vol. 25, no. 4, pp. 905-918, 2008.
- [9] M. Ziabari, V. Mottaghtalab, S. T. McGovern, and A. K. Haghi, "Measuring Electrospun Nanofiber Diameter: a Novel Approach", *Chinese. Phys. Lett.*, vol. 25, no. 8, pp. 3071-3074, 2008.
- [10] M. Maleki, M. Latifi, and M. Amani-Tehran, "Definition of Structural Features of Nano Coated Webs by Image Processing Methods", *Int. J. Nanotechnol.*, vol. 6, no. 1-2, pp. 1131-1154, 2009.
- [11] E. Tomba, P. Facco, M. Roso, M. Modesti, F. Bezzo, and M. Barolo, "Artificial Vision System for the Automatic Measurement of Interfiber Pore Characteristics and Fiber Diameter Distribution in Nanofiber Assemblies", *Ind. Eng. Chem. Res.*, vol. 49, no. 6, pp. 2957-2968, 2010.
- [12] M. Kanafchian, M. Valizadeh, and A. K. Haghi, "Prediction of Nanofiber Diameter For Improvements In Incorporation of Multilayer Electrospun Nanofibers", *Korean. J. Chem. Eng.*, vol. 28, no. 3, pp. 751-755, 2011.
- [13] C. Zeyun, W. Rongwu, Z. Xianmiao, and Y. Baopu, "Study on Measuring Microfiber Diameter in Melt-blown Web Based on Image Analysis", *Procedia Eng.*, vol. 15, pp. 3516-3520, 2011.
- [14] N. Hotaling, K. Bharti, H. Kriel, and C. Simon, "Diameter J: A validated open source nanofiber diameter measurement tool", *Biomaterials*, vol. 61, pp. 327-338, 2015.
- [15] M. Ziabari, V. Mottaghtalab, and A. K. Haghi, "Application of Direct Tracking Method For Measuring Electrospun Nanofiber Diameter", *Braz. J. Chem. Eng.*, vol. 26, no. 1, pp. 53-62, 2009.
- [16] N. Dehghan, P. Payvandy, and M. A. Tavanaie, "Study on Thresholding Methods Development and Nanofiber Diameter Determination Using Image Processing", *J. Text. Sci. Technol.*, (In Persian), vol. 3, no. 3, pp. 17-28, 2014.
- [17] S. Sivanand, "Adaptive Local Threshold Algorithm and Kernel Fuzzy C-Means Clustering Method for Image Segmentation", *Int. J. Latest Trends Eng. Technol.*, vol. 2, pp. 38-42, 2013.
- [18] J. H. Lee and S. I. Yoo, "An Effective Image Segmentation Technique for the SEM Image", *ICIT. IEEE International Conference on Industrial Technology*, China, pp. 1-5, 2008.
- [19] N. Dehghan, P. Payvandy, and M. A. Tavanaie, "Nanofiber Images Thresholding based on Imperial Competitive Algorithm", *Int. J. Comput. Appl.*, vol. 99, no. 6, pp. 37-41, 2014.
- [20] J. C. Bezdek, *Pattern Recognition with Fuzzy Objective Function Algorithms*, New York: Plenum, 1981, pp. 191-203.
- [21] S. Ghosh, S. K. Dubey, "Comparative Analysis of K-means And Fuzzy C-means Algorithms", *Int. J. Adv. Comput. Sci. Appl.*, vol. 4, no. 4, pp. 34-39, 2013.
- [22] R. Nock and F. Nielsen, "Statistical region merging", *Pattern. Anal. Mach. Intell.*, IEEE Transactions, vol. 26, no. 11, pp. 1452-1458, 2004.
- [23] N. Dehghan, "A Study of Draw Ratio Effect on Morphological Properties of Extracted Nanofibers From PP/ PBT BlendFibers Using Image Processing Method (in Persian)", *M.Sc. thesis*, Dept. Text. Eng., Yazd University, Iran, 2014.
- [24] B. Pourdeyhimi, R. Ramanathan, and R. Dent, "Measuring Fiber Orientation in Nonwovens Part I: Simulation", *Text. Res. J.*, vol. 66, no. 11, pp. 713-722, 1996.
- [25] B. Pourdeyhimi, R. Dent, and H. Davis, "Measuring Fiber Orientation in Nonwovens Part III: Fourier Transform", *Text. Res. J.*, vol. 67, no. 2, pp. 143-151, 1997.
- [26] R. Chhabra, "Nonwoven Uniformity-Measurements Using Image Analysis", *Int. Nonwoven J.*, vol. 12, no. 1, pp. 43-50, 2003.
- [27] B. Xu, "Measurement of Pore Characteristics in Nonwoven Fabrics Using Image Analysis", *Cloth. Text. Res. J.*, vol. 14, no. 1, pp. 81-88, 1996.
- [28] A. H. Aydilek, S. H. Oguz, and T. B. Edil, "Digital Image Analysis to Determine Pore Opening Size Distribution of Nonwoven Geotextiles", *J. Comput. Civil Eng.*, vol. 16, no. 4, pp. 280-290, 2002.
- [29] M. Ziabari, V. Mottaghtalab, and A. K. Haghi, "Evaluation of Electrospun Nanofiber Pore Structure Parameters", *Korean. J. Chem. Eng.*, vol. 25, no. 4, pp. 923-932, 2008.
- [30] S. Bansal and R. Maini, "A Comparative Analysis of Iterative and Ostu's Thresholding Techniques", *Int. J. Comput. Appl.*, vol. 66, no. 12, pp. 45-47, 2013.
- [31] W. Niblack, *An Introduction to Digital Image Processing*, Prentice-Hall, Englewood Cliffs, 1986, pp. 115-116.
- [32] J. B. MacQueen, "Some Methods for classification and Analysis of Multivariate Observations", *Proceedings of 5-th Berkeley Symposium on Mathematical Statistics and Probability*, Berkeley, University of California Press, vol. 1, no. 14, pp. 281-297, 1967.
- [33] J. C. Bezdek, L. O. Hall, and L. Clarke, "Review of MR Image Segmentation Techniques Using Pattern Recognition". *Med. Phys.*, vol. 20, no. 4, pp. 1033-1048, 1992.
- [34] J. C. Bezdek, "Cluster Validity with Fuzzy Sets", *J. Cybernetics*, vol. 3, pp. 58-73, 1973.
- [35] Y. Fukuyama and M. Sugeno, "A New Method of Choosing The Number of Clusters For The Fuzzy c-means Method" *In Proc. 5th Fuzzy Syst. Symp.*, Vol. 247, In Japanese, pp. 247-250, 1989.
- [36] X. L. Xie and G. Beni, "A Validity Measure for Fuzzy Clustering". *IEEE Trans. Pattern Anal. Mach. Intell.*, vol. 13, 841-847, 1991.
- [37] K. L. Wu and M. S. Yang, "A cluster validity index for fuzzy clustering", *Pattern. Recogn. Lett.*, vol. 26, no. 9, pp. 1275-1291, 2005.
- [38] J. C. Dunn, "Well-separated clusters and optimal fuzzy partitions", *J. Cybernetics.*, vol. 4, no. 1, pp. 95-104, 1974.
- [39] D. L. Davies and D. W. Bouldin, "A Cluster Separation Measure", *IEEE Trans. Pattern Anal. Mach. Intell.* vol. 2, pp. 224-227, 1979.
- [40] S. C. Sharma, *Applied Multivariate Techniques*, John Wiley and Sons Publication, New York, NY, USA, pp. 185-228, 1996.
- [41] M. Halkidi, Y. Batistakis, and M. Vazirgiannis, "On Clustering Validation Techniques", *J. Intell. Inf. Syst.*, vol. 17, no. 2, pp. 107-145, 2001.
- [42] Z. Wang, A. C. Bovik, H. R. Sheikh, and E. P. Simoncelli, "Image Quality Assessment: From Error Visibility to Structural Similarity", *IEEE Trans. Image Process.* vol. 13, no. 4, pp. 600-612, 2004.
- [43] R. C. Gonzalez and R. E., Woods, *Digital image processing*, 2nd Ed., Prentice Hall, New Jersey, 2001, pp. 450-455.
- [44] B. Jahne, *Digital image processing*, 5th Ed., Springer, Germany, 2002, pp. 245-280.
- [45] Q. Z. Ye, "The signed Euclidean distance transform and its applications", *Proceedings of the 9th International Conference on Pattern Recognition, Rome, Italy*, pp. 495-499, 1988.
- [46] N. Hotaling, K. Bharti, H. Kriel, and C. Simon, "Dataset for the validation and use of Diameter J an open source nanofiber diameter measurement tool", *Data in Brief*, vol. 5, pp. 13-22, 2015.